Science Bulletin 70 (2025) 29–32

Contents lists available at ScienceDirect

Science Bulletin

journal homepage: www.elsevier.com/locate/scib

Short Communication

Daytime radiative freezing

Yi Zhang [a], Chenglong She [a], Jingjing Chen [a], Kui Lai [b], Keqiao Li [c], Fan Yang [a], Chenxi Wang [a], Baoling Huang [c], Lihua Shen [b], Xiaobo Yin [a,d,*]

[a] Department of Mechanical Engineering, The University of Hong Kong, Hong Kong 999077, China
[b] MOE Key Laboratory for Nonequilibrium Synthesis and Modulation of Condensed Matter, School of Physics, Xi'an Jiaotong University, Xi'an 710000, China
[c] Department of Mechanical and Aerospace Engineering, The Hong Kong University of Science and Technology, Hong Kong 999077, China
[d] Department of Physics, The University of Hong Kong, Hong Kong 999077, China

ARTICLE INFO

Article history:
Received 24 July 2024
Received in revised form 13 August 2024
Accepted 11 October 2024
Available online 17 October 2024

While modern refrigerators can easily produce ice at any time, Ancient Persians were known to harvest ice from shallow pools without such means. The ice would form on clear nights even when the ambient temperature remained above freezing [1]. The nocturnal ice formation occurs because the water, facing the sky, radiates heat to the cold expanse of space through the transparent atmospheric window between 8 to 13 μm [2,3]. As a result, the temperature of the water could drop below the ambient temperature. However, achieving daytime ice-making under the sunshine remains a captivating and challenging pursuit.

Drawing from recent advancements in daytime terrestrial radiative cooling, it is now possible to achieve sub-ambient cooling during the day by minimizing solar heat gain and maximizing outgoing thermal radiation through the atmospheric window [4–7]. While naturally available materials struggle to meet these stringent requirements, water surprisingly exhibits favourable optical characteristics for daytime radiative cooling, i.e., low solar absorbance and a close-to-unity mid-infrared emissivity. In this study, we demonstrated that water has good daytime radiative cooling properties, and harnessed water to develop a daytime radiative cooler. Most notably, we demonstrate that liquid water, when exposed to the sky during the day and with the ambient temperature still above freezing, can freeze itself without relying on evaporative cooling or the need for additional energy expenditure. Recently, a paper studied the passive desalination driven by the freezing water underneath a radiative cooler [8]. The difference of this study is that we proved that water can be a radiative cooling material itself and cool down to a sub-freezing point both at nighttime and daytime.

The electromagnetic absorption by liquid water is an intriguing topic with many important applications. Fig. 1a shows the water column depths at which 99% of light is absorbed for wavelengths ranging from 0.25 to 25 μm [9]. The significant absorption depth indicates water is inefficient in absorbing solar light. For example, absorbing 99% of blue light requires a water column depth of 93 m. Only a few absorption lines fall within the near-infrared (NIR) range, around 970, 1200, 1450, and 1950 nm [10]. However, the total solar absorbance is relatively low because the overall solar energy within the NIR wavelength range is much lower than that of the visible wavelengths. For the same thickness, a thin film of water has a lower solar absorptivity compared to many radiative cooling materials reported, such polymeric materials of PMMA, PDMS, and PET. On the other hand, water strongly absorbs mid-infrared electromagnetic waves, attributing to intermolecular vibrations. The mid-infrared spectrum of liquid water consists of three main bands: the dominating feature is the stretching motion of covalent OH bonds at 2.94 μm, followed by the $\widehat{HOH}$ bending band at 6.06 μm, and the hydrogen bond libration at 14.81 μm [10]. Therefore, water has been recognized as a highly absorptive and emissive material in mid-infrared for thermal applications such as steam generation [11] and thermal modulation [12]. The combination of low solar absorptivity and high infrared emissivity makes water a promising candidate for daytime radiative cooling. Clearly, solar absorptivity and thermal emissivity of the water are both thickness-sensitive. To create an effective water-based radiative cooler, the thickness of the water film has to be properly determined. In addition, to reject all solar energy through the solar transparent water layer, a bottom reflective mirror made of metallic aluminium ($R_{solar} \sim 0.94$) or silver ($R_{solar} \sim 0.97$) can be used.

The liquid water evaporates in the environment. In order to ensure the cooling effect is solely due to radiative cooling rather

* Corresponding author.
E-mail address: xbyin@hku.hk (X. Yin).

https://doi.org/10.1016/j.scib.2024.10.010

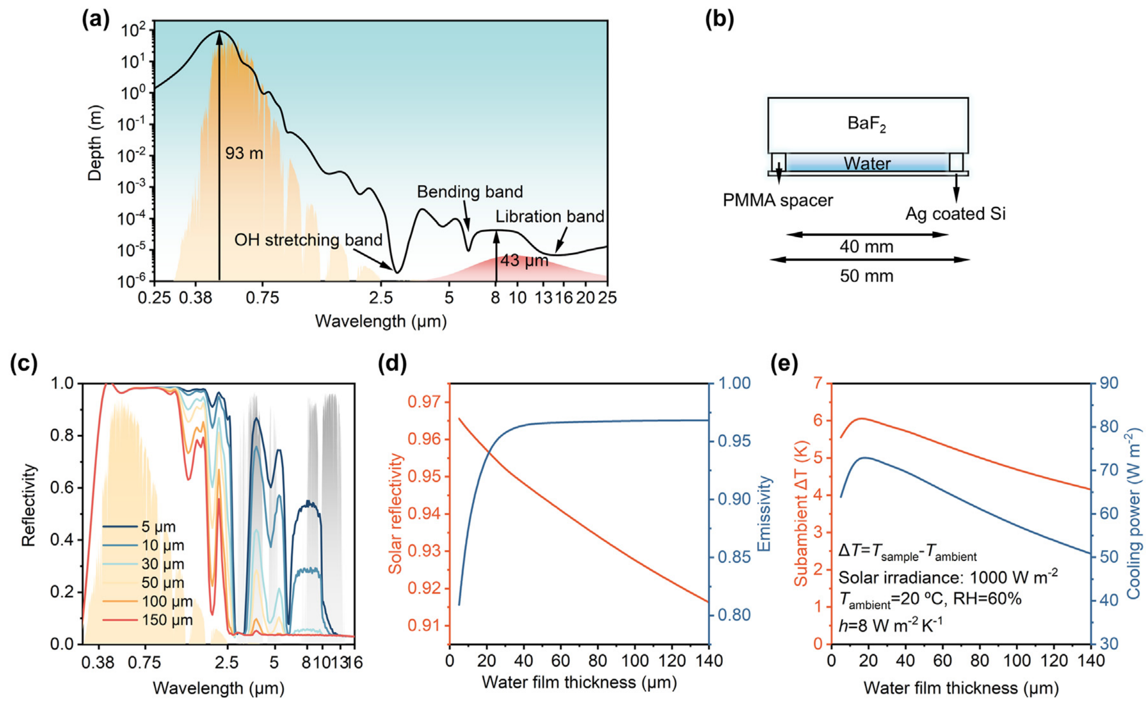

Fig. 1. (a) The penetration depth for 99% absorption for liquid water. The regions shaded in orange and red depict the solar intensity and blackbody thermal emission at 300 K. (b) Side view of the water cooler with dimensions. The structure consists of mid-infrared transparent BaF_2 window, water film, and silver coated silicon wafer. (c) Simulated reflectance spectra of water coolers with different water film thicknesses. (d) The calculated solar reflectivity and emissivity based at different water film thicknesses. (e) The calculated sub-ambient temperature difference and cooling power for water coolers with different water thicknesses.

than evaporative cooling, certain requirements must be met. Firstly, the water must be tightly sealed to prevent evaporation cooling effect. Secondly, the sealing should not interfere with the thermal emission of the water. Thirdly, it is essential to have precise control over the thickness of the water film. Fig. 1b shows the experimental apparatus. The water-based radiative cooler has a sandwich structure comprising a reflective substrate, a liquid water film, and a mid-infrared-transmit cover. To precisely control the water thickness, optically clear acrylic (OCA) double-sided tape of varying thicknesses was employed as a spacer, allowing for water thicknesses ranging from 5 to 150 μm. The reflective substrate needs to be both solar and thermal reflective since we want to compare the cooling effect of different water coolers with different water film thicknesses. Here we use a thermally-evaporated 200 nm-thick silver layer-coated silicon wafer for the purpose of demonstration. As for the cover, the material must be transparent to both visible and infrared light to ensure that the thermal emission of water is not hampered. Barium fluoride (BaF_2) meets these requirements as it remains highly transparent in the spectral range from 0.3 to 13 μm ($T_{400–760\ \mathrm{nm}}$ = 92.9% and $T_{2.5–16\ \mu\mathrm{m}}$ = 96.7% for a 1 mm slice) [13,14]. Moreover, it generally does not react with water, making it an ideal choice for the cooler's cover. Although polyethylene (PE) is also relatively transparent in MIR and does not react with water, the flexibility cannot ensure the precise control of the water film's thickness. The high adhesion of OCA ensures effective sealing of the water between BaF_2 and the silver-coated substrate, preventing water evaporation and evaporative cooling.

The spectral reflectance of the apparatus can be evaluated by employing the plane coherent electromagnetic radiation propagation method, assuming all layers of the materials are stratified [15]. As shown in Fig. 1c, the visible reflectivity remains relatively unchanged within the given thickness ranges due to the high transparency of water to visible light. Two absorption bands are observed in the NIR region at 1.45 and 1.93 μm. Additionally, two broad peaks of reflectivity are observed in the mid-infrared (3–6 μm and 6–13 μm) range. Based on the spectral results, the calculated solar reflectivity and infrared emissivity are shown in Fig. 1d. The solar reflectivity decreases with increasing water thickness, while the infrared emissivity rises and saturates at a water film thickness around 50 μm. Consequently, the optimal water film thickness should be below 50 μm to achieve a balance where the infrared emissivity no longer increases, while the solar reflectivity continues to decrease. The water cooler is a near-blackbody broadband type, as it has a close-to-unity emissivity across the whole infrared spectrum range.

By considering the solar reflectivity and thermal emissivity of water coolers, as well as the calculated atmospheric transmission from MODTRANS, we solved Eq. S1 in the Supplementary materials to determine the steady-state temperature of water coolers with different water thickness under specific weather conditions (air temperature of 8 °C, relative humidity of 40%, solar intensity of 600 W m^{-2}, and convective heat transfer coefficient of 8 W m^{-1} K^{-1}). The results are depicted in Fig. 1e. It is observed that both the sub-ambient temperature difference and cooling power initially experience a rapid increase, followed by a gradual decline as the water film thickness increases. The initial growth is due to the increased thermal emissivity, while the subsequent decrease is a result of the higher solar absorptivity of the water film. The optimal water thickness is approximately 20 μm, where the water cooler achieves a sub-ambient cooling of 6 °C and the highest cooling power of 72 W m^{-2}. An overly thick or thinner water cooler reduces the performance. As shown in Fig. 1e, the cooler with a water thickness of 20 μm exhibits the best performance under this weather condition, for example, registering a temperature difference of approximately 1 °C compared to coolers with 5 or 50 μm

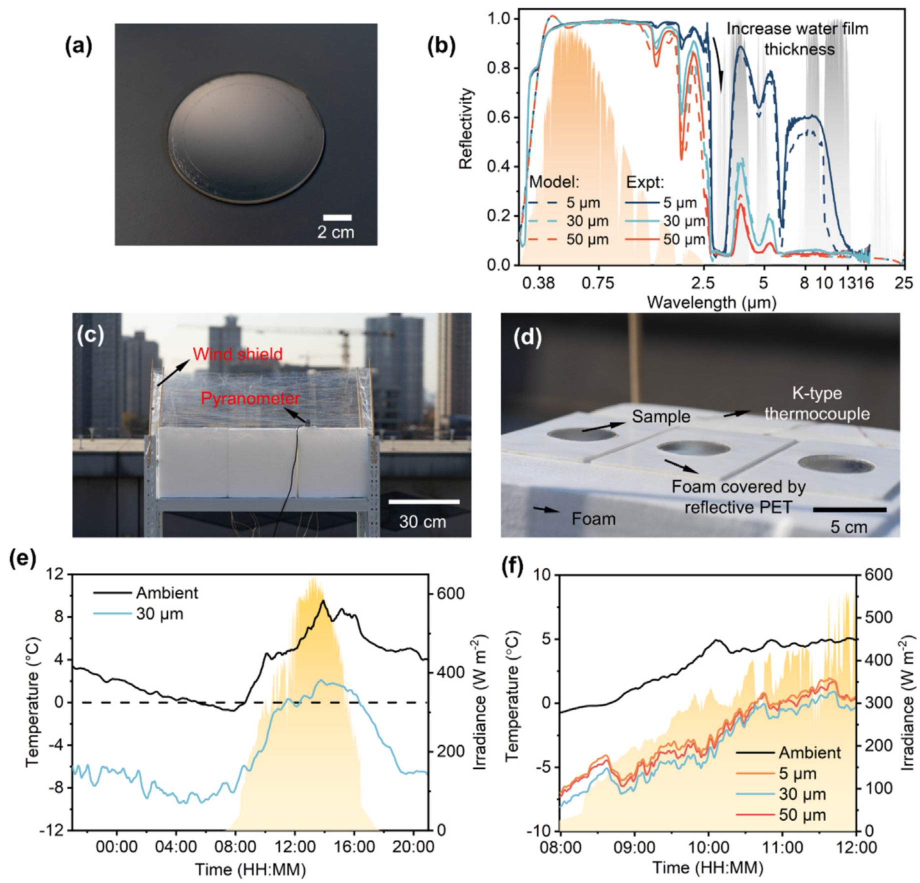

Fig. 2. (a) Photograph of water cooler. (b) Reflection spectra of the fabricated water coolers and the comparison with theoretical results. (c, d) Experimental setup for characterizing the sub-ambient cooling of water cooler and daytime ice-making. The polyethylene film was served as a windshield to reduce the convective heat loss. The pyranometer was placed next to the samples to monitor the solar irradiance in real time. (e) Sample temperatures, ambient air temperature, and solar intensity were measured in Xi'an over 24 h from November 30, 2023 to December 1, 2023. Dashed line: Freezing point. (f) The temperatures of coolers with different water thickness (5, 30, and 50 μm) and ambient air on December 1, 2023.

thicknesses. We subsequently fabricated the water cooler as shown in Fig. 2a. Three different thicknesses (5, 30, and 50 μm) were chosen based on the available spacers. The spectral results of the samples were obtained using the UV–VIS-NIR spectrometer and FTIR, covering a wavelength range from 300 nm to 16 μm, as shown in Fig. 2b. The experimental measurements agreed well with the theoretical predictions.

We conducted experimental demonstrations of the sub-ambient cooling of the water cooler and the passive daytime ice-making in Xi'an, Shaanxi, China. The experimental setup is illustrated in Fig. 2c and d. The samples were directly mounted on a cubic, high-density expanded polystyrene (EPS) foam. The EPS foam possesses high solar reflectivity and low thermal conductivity, minimizing the heat absorbed by the foam and its heat transfer to the samples. Thermocouples were inserted between the coolers and the foam, measuring the temperature of the cool substrate, as shown in Fig. S1 (online). Since the lower side of the samples was well-insulated and the substrate was in excellent thermal contact with water, the substrate temperature effectively represented the water temperature. To ensure accurate measurement of the ambient air temperature, precautions were taken to avoid heating from the ground and direct exposure of the thermometer to sunlight. A properly calibrated commercial weather station was employed, equipped with a shutter box. The weather station was used to measure the ambient air temperature, relative humidity, solar irradiation, and wind speed simultaneously. The cooler sidewalls were insulated with foam to minimize heat loss and double-layered infrared-transparent polyethylene films were placed vertically around the samples, serving as windshields and preventing convective heat transfer.

The measured temperatures of the water cooler along with the ambient temperatures and solar irradiation are presented in Fig. 2e. During the test period, (from November 31, 2023, to December 1, 2023), the sky was clear with no visible clouds. Throughout the 24-hour, the water cooler consistently maintained a temperature lower than that of the ambient air. Additionally, the water temperature remained below freezing for most of the day, even when the ambient temperature exceeded 0 °C. The highest temperature recorded for the water cooler was 2 °C at 14:00, while the air temperature was 8 °C. The maximum sub-ambient temperature difference reached 12 °C at dusk when both relative humidity and solar intensity were low (Fig. S2a online) while the minimum temperature difference was 4 °C, recorded at noon. Detailed measurements of relative humidity, wind speed, and the temperature difference between water coolers and ambient are shown in Fig. S2b (online). When the liquid water film reaches below the freezing point, it transforms into a solid ice layer. Ice, compared to water, exhibits a greater clarity in the visible range while maintaining a similar thermal emissivity [9]. That means that after the water film freezes into ice, it continues to function as a high-performance daytime radiative cooler with high solar reflectivity and thermal emissivity. However, due to the ultrathin thickness of the water film, it is difficult to visualize the ice formation or the ice cubes.

To validate the impact of water layer thickness on cooling performance, we conducted comparative experiments with water coolers of varying thicknesses (5, 30, and 50 μm). As shown in Fig. 2f, all three water coolers achieved sub-ambient cooling. Notably, the water cooler with 30 μm-thick water film exhibited the highest temperature reduction. The water coolers with 5 and 50 μm thicknesses show similar temperature trends. These results are consistent with the predictions illustrated in Fig. 1e.

Liquid water, the most common naturally available substance, has never been explored as a daytime radiative cooling material. Liquid water possesses superior optical properties (low solar absorption and high thermal emissivity) when compared to most materials specifically synthesized for radiative coolers. By controlling the water film thickness, in our study, the cooler demonstrated optimal solar reflectivity of 96% and thermal emissivity of 0.94. A 24-hour continuous field test confirmed its sub-ambient cooling performance and demonstrated daytime radiative cooling ice-forming is possible under direct sunshine while the ambient temperature is greater than zero. However, due to the limited cooling power of the daytime radiative cooler, the ambient temperature for the water in the water cooler to freeze should be below about 6 °C.

Conflict of interest

The authors declare that they have no conflict of interest.

Acknowledgments

This work was supported by the Hong Kong Jockey Club Charities Trust, New Cornerstone Science Foundation through the XPLORER Prize, and the Hong Kong Research Grants Council through Grant No. C5051-22GF.

Author contributions

Yi Zhang conceived the idea, performed the fabrication and demonstration, and wrote and revised the manuscript. Chenglong She performed the optical characterizations. Jingjing Chen conducted the simulations. Kui Lai designed the outdoor experiment setup. Keqiao Li, Fan Yang, and Chenxi Wang analyzed the data. Baoling Huang, Lihua Shen, and Xiaobo Yin supervised the project. All authors discussed the results and commented on the manuscript at all stages.

Appendix A. Supplementary material

Supplementary data to this article can be found online at https://doi.org/10.1016/j.scib.2024.10.010.

References

[1] Mahdavinejad M, Javanrudi K. Assessment of ancient fridges: a sustainable method to storage ice in hot-arid climates. Asian Cult Hist 2012;4:133.
[2] Granqvist C, Hjortsberg A. Radiative cooling to low temperatures: general considerations and application to selectively emitting SiO films. J Appl Phys 1981;52:4205–20.
[3] Raman AP, Anoma MA, Zhu L, et al. Passive radiative cooling below ambient air temperature under direct sunlight. Nature 2014;515:540–4.
[4] Yin X, Yang R, Tan G, et al. Terrestrial radiative cooling: using the cold universe as a renewable and sustainable energy source. Science 2020;370:786–91.
[5] Lee G, Kang H, Yun J, et al. Integrated triboelectric nanogenerator and radiative cooler for all-weather transparent glass surfaces. Nat Commun 2024;15:6537.
[6] So S, Yun J, Ko B, et al. Radiative cooling for energy sustainability: from fundamentals to fabrication methods toward commercialization. Adv Sci 2024;11:2305067.
[7] Yun J, Chae D, So S, et al. Optimally designed multimaterial microparticle–polymer composite paints for passive daytime radiative cooling. ACS Photonics 2023;10:2608–17.
[8] Huang X, Mandal J, Xu J, et al. Passive freezing desalination driven by radiative cooling. Joule 2022;6:2762–75.
[9] Hale GM, Querry MR. Optical constants of water in the 200-nm to 200-μm wavelength region. Appl Opt 1973;12:555–63.
[10] Modest MF, Mazumder S. Radiative Heat Transfer. Academic press; 2021.
[11] Menon AK, Haechler I, Kaur S, et al. Enhanced solar evaporation using a photo-thermal umbrella for wastewater management. Nat Sustain 2020;3:144–51.
[12] Lin C, Hur J, Chao CY, et al. All-weather thermochromic windows for synchronous solar and thermal radiation regulation. Sci Adv 2022;8:eabn7359.
[13] Querry MR. Optical constants of minerals and other materials from the millimeter to the ultraviolet. (US Army Report CRDECCR-88009, 1987); 1998, https://apps.dtic.mil/sti/pdfs/ADA192210.pdf.
[14] Jia Y, Liu D, Chen D, et al. Transparent dynamic infrared emissivity regulators. Nat Commun 2023;14:5087.
[15] Hansen WN. Electric fields produced by the propagation of plane coherent electromagnetic radiation in a stratified medium. J Opt Soc Am 1968;58:380–90.